Journal of Applied Fluid Mechanics, Vol. 9, No. 6, pp. 2823-2836, 2016.
Available online at www.jafmonline.net, ISSN 1735-3572, EISSN 1735-3645.

Conjugate Effect of Joule Heating and Unsteady MHD Natural Convection in a Differentially Heated Skewed Porous Cavity Saturated by *Cu*-water Nanofluid

O. Ghaffarpasand

Department of Physics, University of Isfahan, Isfahan, Iran

Email: O.ghaffarpasand@gmail.com

(Received December 14, 2015; accepted April 24, 2016)

ABSTRACT

Conjugate effect of Joule heating and Lorentz force in a differentially skewed porous lid-driven cavity saturated by Cu-water nanofluid have been examined numerically. A coordinate transformation is utilized to transform the physical domain to the computational domain in an orthogonal coordinate. The Darcy-Brinkman-Forchheimer model with Boussinesq approximation is adopted and the developed mathematical model is solved by finite volume method based on SIMPLE algorithm. The influence of porous medium permeability (Darcy number), Joule heating (Eckert number), nanoparticle volume fraction, as well as inclination angle of skewed cavity on fluid flow and heat transfer characteristics are studied. The entropy generation and Bejan number also evaluated to examine thermodynamic optimization of the MHD mixed convection in porous media. The results have been presented in terms of streamlines, average Nusselt number, entropy generation, and Bejan number for a wide range of key parameters.

Keywords: Skewed cavity; MHD mixed convection; Porous media; Nanofluid; Heat transfer; Entropy generation.

NOMENCLATURE

Be	Bejan Number
B_0	magnetic field intensity
Da	Darcy number
Ec	Eckert number
g	gravitational acceleration
Ha	Hartmann number
Nu	local Nusselt number
p	pressure
Pr	Prandtl number
Re	Reynolds number
Ri	Richardson number
S	average entropy generation
U_0	upper wall velocity
Gr	Grashof number
L	enclosure length
K	thermal conductivity
x,y	dimensionless Cartesian coordinates
α	thermal diffusivity
β	coefficient of thermal expansion
η	transformation coordinate in y-direction
ε	porosity
μ	dynamic viscosity
ν	kinematic viscosity
ρ	density
σ	electrical conductivity
Θ	dimensionless temperature
Φ	solid volume fraction
ζ	transformation coordinate in x-direction

Subscript

f	pure fluid
S	solid
nf	nanofluid

1. INTRODUCTION

The speciality which studies natural convection in lid-driven cavities is of considerable interest in the modern systems of practical importance (Bhattacharya and Das, 2015). Due to the energy dissipation, operating noise, and less reliability of the mechanical equipment involving fluid circulation, forced convection, application of natural convection based heat exchangers are more preferable.

However, traditional convectional fluids such as water, oil, and ethylene glycol have usually low

thermal conductivity (Moraveji and Hejazian, 2013). To overcome this obstacle, new technique emerges, which consists of introducing minor volume fraction of solid metallic nanoparticles with higher thermal conductivity and size up to 1-100 nm in the base fluid. The product called nanofluid by Choi (1995).

Different type of nanofluids are available commercially, among them, Al_2O_3 / TiO_2 / Cu - water are very common (Malvandi *et al*. 2014). The problem of convective heat transfer inside the cavities filled by nanofluids has been extensively studied by many researchers in recent years. Muthtamilselvan *et al*. (2010) performed numerical study to characterize convective heat transfer of *Cu*-water nanofluid in a lid-driven cavity. Results demonstrate that the volume fraction of metallic nanoparticles developed sufficiently heat transfer along the cavity. Muthtamilselvan and Doh (2014) carried out another numerical study to research steady mixed convection of *Cu*-water nanofluid inside a lid-driven cavity. They observed that Richardson number has influenced enough heat transfer across the cavity. AbuNada and Chamkha (2014) investigated steady laminar mixed convection flow in a driven cavity with a wavy wall filled with Cu-water nanofluid. Results show that the presence of nanoparticles improve heat transfer of various regime of convection. Sheremet and Pop (2014) studied numerically mixed convection in a two-sided lid-driven cavity filled with water based nanofluid. They analyzed the effects of Prandtl and Lewis numbers on fluid flow and heat transfer. Moumni *et al*. (2015) utilized numerical model to study nanofluid mixed convection in a two-sided lid-driven cavity including discrete heat sources. Their results show that the place of heating source in addition to nanoparticle material are important factors which can influence enough heat transfer inside the cavity.

However, all of above studies were performed in non-porous medium, while there has been considerable renewed interest in studying flow in porous media in recent years. Problem of natural convection in porous media have several engineering applications such as geothermal energy recovery, crude oil extraction, thermal energy storage and many others (Nield and Bejan, 2013, Shermet *et al*. 2015, Ghalambaz *et al*. 2015, Astanina *et al*. 2015). One of the innovative technique to control natural convection in porous media is applying an external magnetic filed, named magnetohydrodynamic (MHD) natural convection (Abbasian Arani *et al*. 2014, Loganthan and Vimala, 2015, Mohammadi and Rashidi, 2016). Actually, Lorentz force makes an additional resistance against fluid motion, whereby slows down fluid intensity and reduces convection heat transfer. MHD natural convection flow in a porous enclosure has taken a great interest recently due to its wide and various applications in science and engineering such as cooling of nuclear reactors, MHD accelerators and generators, thermal insulation systems, optimization of solidification processes of metals and alloys, design of MHD power generators and etc (Pekman and Tezer-Sezgin, 2014, Fersadou *et al*. 2015). On the literature survey of this subject, Suneetha *et al*. (2011) performed numerical simulations to study MHD natural convection flow inside a cavity. Results proved that fluid flow and isotherm contours are significantly influence by external magnetic field. Makinde (2012) looked into the problem of hydromagnetic mixed convection stagnation point flow past a vertical plate embedded in a highly porous medium in the presence of thermal radiation and internal heat generation. Results proved that both heat and mass transfer improve with the enhancement of external magnetic field and radiation parameters. Sahoo *et al*. (2013) analytically studied laminar MHD mixed convection stagnation point flow and heat transfer on a heated semi-infinite permeable surface embedded in a porous medium. He found that the presence of porous matrix is ineffective to modify the velocity field. Later, Pekmen and Tezer-Sezgin (2014) performed a numerical investigation to examine MHD flow and heat transfer in a lid-driven porous enclosure. Results explored that decrease in Darcy number and increase in Hartmann number suppressed the fluid flow and heat transfer.

The study of MHD convection of nanofluids in porous media has also attracted the interest of many researchers, especially in recent years. Murthy *et al*. (2013) researched the effect of magnetic field on flow, heat and nanoparticles mass transfer characteristics in free convection along a vertical plate immersed in a porous medium saturated by a thermally stratified nanofluid. Sheikholeslami *et al*. (2013) carried out numerical simulations to examine laminar MHD convection of nanofluid in a semi-porous channel. Results indicate that the strength of external magnetic field in addition to solid volume fraction significantly influenced fluid flow and heat transfer. Servati *et al*. (2014) utilized the Lattice Boltzmann Method (LBM) to examine forced convection flow in a channel partially filled with a porous medium saturated by a nanofluid. Heat transfer across the channel improved by further increasing of external magnetic field and solid volume fraction.

In most of the studies mentioned above, the influence of internal joule heating, which is an important factor in heat transfer and fluid flow seems to be neglected. Moreover, although some studies on MHD convection of nanofluid inside a porous cavity are available, the corresponding research analyzing entropy generation is quite sparse. However, Entropy Generation Minimization (EGM) can be an optimal design criteria for thermal systems (Nayak *et al*. 2015). Entropy generation of Cu-water nanofluid flow over an inclined transparent plate embedded in a porous medium was investigated by Dehsara *et al*. (2014). The authors considered the effects of solar radiation, viscous dissipation and variable magnetic field, but still neglected the influence of internal joule heating. Fersadou *et al*. (2015) con-ducted a numerical study to examine entropy generation and MHD mixed convection of a nanofluid in a vertical porous channel. They actually did not research the effect of joule heating, because a certain value of Eckert numbers assumed during their simulations. Its also worthwhile to note that whole of the above studies carried out in square or rectangular cavities,

while, to author best knowledge, the problem of heat transfer enhancement of MHD natural convection in a skewed porous cavity has not been studied yet. The constrain due to complex geometry of the skewed cavity makes the problem of the MHD natural convection difficult as compared to a square enclosure.

In this article, MHD natural convection conjugated by internal joule heating in a porous skewed cavity saturated by *Cu*-water nanofluid has been studied numerically. This study also aims to characterize the heat transfer and fluid flow due to addition of metallic nanoparticles at different flow configurations. Moreover, a quantitative study conducted to analyze entropy generation and effective factors affected on fluid irreversibilities. The flow fields and the rates of heat transfer and entropy production are graphically illustrated for different key parameters.

Table 1. Thermo-physical properties of pure water and copper nanoparticles.

Physical properties	Pure water	Cooper
p(kgm^{-3})	997	8933
Cp(Jkg^{-1}K^{-1})	4179	385
k(Wm^{-1}K^{-1})	0.613	401
β*10^{-5}(K^{-1})	21	1.67
σ(Sm^{-1})	0.05	5.96*10^{7}

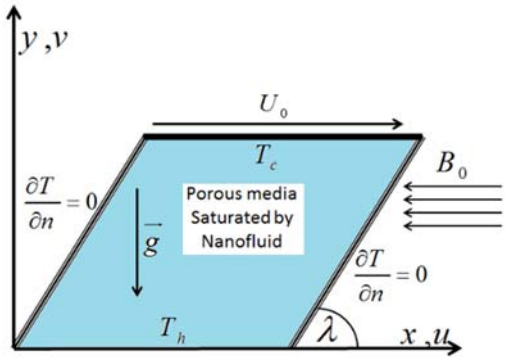

Fig. 1. Schematic configuration of the studied problems.

2. PROBLEM STATEMENT

A schematic geometry of the present problem is shown in Fig. 1. It consists of two-dimensional porous skewed cavity whose bottom wall is along the x-axis and side walls make an angle λ with x-axis. Top and bottom walls are hot and cold walls respectively, while the others are assumed to be adiabatic. Top wall also moves with uniform and constant velocity U_0 . The porous media of the cavity saturated by nanofluid, whereby both the fluid phase and the nanoparticles are in thermal equilibrium and flow at the same velocity. The nanofluid is Newtonian, incompressible, and laminar, and the porous medium is hydrodynamically, thermally and electrically isotropic in the local thermal equilibrium with the nanofluid. The thermo-physical properties of utilized nanofluid are given in Table 1. It was assumed that nanoparticles suspended in nanofluid is smaller enough than matrix pores and agglomeration and deposition of those nanoparticles on the porous matrix is negligible. The thermo-physical properties of the porous medium, the base fluid, and the nanoparticles are assumed to be constant except the density in the buoyancy term, which obeys the Boussinesq approximation. Meanwhile, the radiated heat transfer and the chemical reaction between the base fluid and nanoparticles are neglected. The viscous dissipation and Hall effect are all assumed negligible. An external magnetic field is applied in the x-direction. Besides, it is assumed that there is no any applied voltage which implies the absence of an electric field. Based on the above hypothesis and adopting the nanofluid model proposed by Tiwari and Das (2007) along with the Brinkman-Forchheimer extended Darcy model (Vafai and Tien, 1981) to in-corporate the viscous and inertia effects, the governing equations in vector form are as follows:

$$\vec{\nabla}.\vec{V}=0 \tag{1}$$

$$\frac{\rho_{nf}}{\varepsilon^2}\vec{V}\vec{\nabla}\vec{V}=\vec{\nabla}p+\frac{\mu_{eff}}{\varepsilon}\nabla^2\vec{\nabla}-\frac{\mu_{eff}}{K}\vec{V}-\rho_{nf}\frac{C}{\sqrt{K}}\left|\vec{V}\right|\vec{V}-(\rho\beta)_{nf}(T-T_c)\vec{g}+\vec{f}\times\vec{B} \tag{2}$$

$$(\rho C_p)_{nf}\vec{V}\vec{\nabla}T=K_{eff}\nabla^2T+\frac{J^2}{\sigma_{nf}} \tag{3}$$

Where $\frac{J^2}{\sigma_{nf}}$ is the energy dissipated by joule heating. The governing equation in non-dimensional form can be expressed as:

$$\frac{\partial u}{\partial x}+\frac{\partial v}{\partial y}=0 \tag{4}$$

$$\frac{\partial u}{\partial \tau}+\frac{\partial(uu)}{\partial x}+\frac{\partial(uv)}{\partial y}=-\frac{\partial p}{\partial x}+\frac{\rho_f}{\rho_{nf}}\frac{1}{(1-\phi)^{2.5}}\frac{R_\mu}{Re}\left(\frac{\partial^2u}{\partial x^2}+\frac{\partial^2u}{\partial y^2}\right)-\frac{\rho_f}{\rho_{nf}}\frac{1}{(1-\phi)^{2.5}}\frac{\varepsilon}{ReDa}u-\frac{\varepsilon^2C}{\sqrt{Da}}\left|\vec{V}\right|u \tag{5}$$

$$\frac{\partial v}{\partial \tau}+\frac{\partial(uv)}{\partial x}+\frac{\partial p(vv)}{\partial y}=-\frac{\partial p}{\partial y}+\frac{\rho_f}{\rho_{nf}}\frac{1}{(1-\phi)^{2.5}}\frac{R_\mu}{Re}\left(\frac{\partial^2v}{\partial x^2}+\frac{\partial^2v}{\partial y^2}\right)-\frac{\rho_f}{\rho_{nf}}\frac{1}{(1-\phi)^{2.5}}\frac{\varepsilon}{ReDa}v-\frac{\varepsilon^2C}{\sqrt{Da}}\left|\vec{V}\right|u-\frac{\varepsilon Ha^2v}{Re}\frac{\rho_f}{\rho_{nf}}\frac{\sigma_{nf}}{\sigma_f}+\frac{(\rho\beta)_{nf}}{(\rho\beta)_f}\frac{\rho_f}{\rho_{nf}}Ri\Theta \tag{6}$$

$$\frac{\partial\Theta}{\partial\tau}+\frac{\partial(u\Theta)}{\partial x}+\frac{\partial(v\Theta)}{\partial y}=$$
$$\frac{R_k}{\varepsilon RePr}\frac{k_{nf}}{k_f}\frac{(\rho C_p)_{nf}}{(\rho C_p)_f}\left(\frac{\partial^2\Theta}{\partial x^2}+\frac{\partial^2\Theta}{\partial y^2}\right)+ \quad (7)$$
$$\frac{\varepsilon \mathrm{Ec} Ha^2}{Re}\frac{(\rho C_p)_{nf}}{(\rho C_p)_f}\frac{\sigma_{nf}}{\sigma_f}v^2$$

The governing equations were non-dimensionalized using the following dimensionless variables:

$$(x,y)=\frac{(x',y')}{L},\quad (u,v)=\frac{(u',v')}{\varepsilon U_0},\quad \Theta=\frac{T-T_c}{T_h-T_c},$$
$$\tau=\frac{t\varepsilon U_0}{L},\quad P=\frac{p}{\rho_{nf}U_0^2}$$

where variables with subscript $'$ are in dimensional form. The effective density at the reference temperature, thermal diffusivity, heat capacitance and thermal expansion coefficient of the nanofluids based on classical models can be written as follows (Mejri *et al*. 2014, Moumni *et al*. 2015):

$$\rho_{nf}=(1-\phi)\rho_f+\phi\rho_s \quad (8)$$

$$\alpha_{nf}=\frac{k_{nf}}{(\rho C_p)_{nf}} \quad (9)$$

$$(\rho C_p)_{nf}=(1-\phi)(\rho C_p)_f+\phi(\rho C_p)_s \quad (10)$$

$$(\rho\beta)_{nf}=(1-\phi)(\rho\beta)_f+\phi(\rho\beta)_s \quad (11)$$

where ϕ is the solid volume fraction of the nanoparticles. The effective thermal conductivity of nanofluid is approximental by the Maxwell self-consistent approximation model, whereby for the two-component entity of spherical-particle suspension, k_{nf} can be expressed as (Mejri *et al*. 2014, Moumni *et al*. 2015):

$$\frac{k_{nf}}{k_f}=\frac{k_s+2k_f-2\phi(k_f-k_s)}{k_s+2k_f+2\phi(k_f-k_s)} \quad (12)$$

The viscosity of the nanofluid is calculated using the Brinkman model as:

$$\mu_{nf}=\frac{\mu_f}{(1-\phi)^{2.5}} \quad (13)$$

The electrical conductivity of the nanofluid calculated by Maxwell model as:

$$\frac{\sigma_{nf}}{\sigma_f}=1+\frac{3(\xi-1)\phi}{(\xi+2)-(\xi-1)\phi} \quad (14)$$

where $\xi=\frac{\sigma_s}{\sigma_f}$. The boundary conditions associated with the problem in physical domain are as follows:

$u=1, v=0,\ \Theta=-0.5$ *for* $y=\sin\lambda$, *and* $\cos\lambda\le x\le\cos\lambda+1$ (*Top wall*)

$u=v=0,\ \Theta=+0.5$ *for* $y=0$, *and* $0\le x\le 1$ (*Bottom wall*)

$u=v=0,\ \frac{\partial\Theta}{\partial n}=0,$ *for* $x=y\cos\lambda (0\le y\le 1)$ *and* $0\le y\le\sin\lambda$ (*Left wall*)

$u=v=0,\ \frac{\partial\Theta}{\partial n}=0,$ *for* $x=1+y\cos\lambda (0\le y\le 1)$ *and* $0\le y\le\sin\lambda$ (*Right wall*)

Here n is the normal displacement respect to the left and right side walls. The problem of MHD natural correction characterized here by the following dimensionless parameters:

$$Ri=\frac{Gr}{Re^2}=\frac{g\beta\Delta L^3/\nu_f^2}{(U_0L/\nu_f)^2},\quad Pr=\frac{\nu_f}{\alpha_f},$$
$$Ha=B_0\sqrt{\frac{\sigma_f L}{\mu_f}},\quad \frac{U_0^2}{(C_p)_f\Delta T}$$

Where *Ri, Gr, Re, Pr, Ha,* and *Ec*, are Richardson, Grashof, Reynolds, Hartmann and Eckert numbers, respectively. A coordinate transformation utilized to transfer physical domain in x,y plane into an orthogonal system in the computational domain. For this purpose, similar method to Nayak *et al*. (2015) conducted, whereby independent variables x,y in the physical domain are transformed into the independent variables ζ,η in the computational domain by the following relation:

$$\zeta=x-y\cot\lambda,\quad \eta=y/\sin\lambda \quad (15)$$

Under this transformation, the governing equations are transformed in the computational domain as:

$$\frac{\partial}{\partial\zeta}(u-v\cot\lambda)+\frac{\partial}{\partial\eta}\left(\frac{v}{\sin\lambda}\right)=0 \quad (16)$$

$$\frac{\partial u}{\partial\tau}+\frac{\partial}{\partial\zeta}(uu)-\cot\lambda\frac{\partial}{\partial\zeta}(uv)+\frac{1}{\sin\lambda}\frac{\partial}{\partial\eta}(uv)=$$
$$-\frac{\partial P}{\partial\zeta}+\frac{R_\mu}{\mathrm{Re}}\frac{\mu_{nf}}{\mu_f}\frac{\rho_f}{\rho_{nf}}a\left(\frac{\partial^2u}{\partial\zeta^2}+\frac{\partial^2u}{\partial\eta^2}-2c\frac{\partial^2u}{\partial\zeta\partial\eta}\right)- \quad (17)$$
$$\frac{\varepsilon^2C}{\sqrt{Da}}|V|u-\frac{\mu_{nf}}{\mu_f}\frac{\rho_f}{\rho_{nf}}\frac{\varepsilon}{\mathrm{Re}\,Da}u$$

$$\frac{\partial v}{\partial\tau}+\frac{\partial}{\partial\zeta}(uv)-\cot\lambda\frac{\partial}{\partial\zeta}(vv)+\frac{1}{\sin\lambda}\frac{\partial}{\partial\eta}(vv)=$$
$$-\frac{\partial P}{\partial\eta}+\cot\lambda\frac{\partial P}{\partial\zeta}+\left(1-\frac{1}{\sin\lambda}\right)\frac{\partial P}{\partial\eta}+$$
$$\frac{R_\mu}{\mathrm{Re}}\frac{\mu_{nf}}{\mu_f}\frac{\rho_f}{\rho_{nf}}a\left(\frac{\partial^2v}{\partial\zeta^2}+\frac{\partial^2v}{\partial\eta^2}-2c\frac{\partial^2v}{\partial\zeta\partial\eta}\right)-\frac{\varepsilon^2C}{\sqrt{Da}}|V|u$$
$$-\frac{\mu_{nf}}{\mu_f}\frac{\rho_f}{\rho_{nf}}\frac{\varepsilon}{\mathrm{Re}\,Da}v+\frac{\rho_f}{\rho_{nf}}\frac{(\rho\beta)_{nf}}{(\rho\beta)_f}Ri\Theta-\frac{\varepsilon Ha^2}{\mathrm{Re}}\frac{\rho_f}{\rho_{nf}}\frac{\sigma_{nf}}{\sigma_{nf}}v \quad (18)$$

$$\frac{\partial\Theta}{\partial\tau}+\frac{\partial}{\partial\zeta}(u\Theta)-\cot\lambda\frac{\partial}{\partial\zeta}(v\Theta)+\frac{1}{\sin\lambda}\frac{\partial}{\partial\eta}(v\Theta)=$$
$$\frac{R_k}{\varepsilon\,\mathrm{Re}\,Pr}\frac{k_{nf}}{k_f}\frac{(\rho C_p)_f}{(\rho C_p)_{nf}}a\left(\frac{\partial^2\Theta}{\partial\zeta^2}+\frac{\partial^2\Theta}{\partial\eta^2}-2c\frac{\partial^2\Theta}{\partial\zeta\partial\eta}\right)+$$

$$\frac{\varepsilon \mathrm{Ec} Ha^2}{Re}\frac{(\rho C_p)_f}{(\rho C_p)_{nf}}\frac{\sigma_{nf}}{\sigma_{nf}}v^2 \tag{19}$$

where $a=\mathrm{cosec}^2\lambda$, and $c=\cos\lambda$. Boundary conditions in the computational domain are:

$$\begin{cases} u=1, v=0,\ \Theta=-0.5,\ at\ \eta=1\ (Top\ wall) \\ u=v=0,\ \Theta=0.5\ at\ \ \eta=0\ (Bottom\ wall) \end{cases}$$

$$u=v=0,\ \frac{\partial\Theta}{\partial\zeta}=\cos\lambda\frac{\partial\Theta}{\partial\eta},\ at\ \ \zeta=0\ (Left\ wall)$$

$$u=v=0,\ \frac{\partial\Theta}{\partial\zeta}=\cos\lambda\frac{\partial\Theta}{\partial\eta},\ at\ \ \zeta=1\ (Right\ wall)$$

To examine heat transfer across the cavity local nusselt number *Nu* on hot wall computed. The local nusselt number *Nu* are calculated as:

$$Nu=-\frac{k_{nf}}{k_f}\left(\frac{1}{\sin\lambda}\frac{\partial\Theta}{\partial\eta}-\cot\lambda\frac{\partial\Theta}{\partial\zeta}\right) \tag{20}$$

The average Nusselt number then obtained by:

$$\overline{Nu}=\int_0^1 Nu d\zeta \tag{21}$$

In the studied problem, entropy generation is due to irreversibility generated through heat transfer, fluid friction, internal joule heating and magnetic field (hydromagnetic effect). As a result, the local entropy generation is the sum of irreversibilities due to viscous dissipation, thermal gradients, and magnetic fields. The entropy generation in computational domain and in dimensionless form can be written as:

$$\begin{aligned} S &= S_T+S_F+S_B= \\ &\left(\frac{k_{nf}}{k_n}\right)\left[\left(\frac{\partial\Theta}{\partial\zeta}\right)^2+\left(-\frac{\partial\Theta}{\partial\zeta}\cot\lambda+\frac{\partial\Theta}{\partial\eta}\frac{1}{\sin\lambda}\right)^2\right] \\ &+\chi\frac{\mu_{nf}}{\mu_f}\left[2\left(\left(\frac{\partial u}{\partial\zeta}\right)^2+\left(-\frac{\partial\Theta}{\partial\zeta}\cot\lambda+\frac{\partial\Theta}{\partial\eta}\frac{1}{\sin\lambda}\right)^2\right)+\right. \\ &\left.\left(-\frac{\partial}{\partial\zeta}\left(v-u\cot\lambda\right)+\frac{\partial u}{\partial\eta}\frac{1}{\sin\lambda}\right)^2\right]+ \\ &\chi\frac{\varepsilon}{Da}\frac{\mu_{nf}}{\mu_f}\left(u^2+v^2\right)+\chi\varepsilon^2 Ha^2\frac{\sigma_{nf}}{\sigma_f}v^2 \end{aligned} \tag{22}$$

Here $T_m=(T_h+T_c)/2$ is the reference temperature. In above equation, χ is the irreversibility factor and expressed as (Mehrez *et al*. 2015):

$$\chi=\frac{\mu_f T_m}{k_f}\left(\frac{U_0}{T_h-T_c}\right)^2 \tag{23}$$

The average entropy generation is given as:

$$\overline{S}=\int_0^1\int_0^1 S d\zeta d\eta \tag{24}$$

To examine the irreversibility distribution, average Bejan number $\overline{Be}$ reported as (Bejan, 1979):

$$\overline{Be}=\int_0^1\int_0^1\left(Be=\frac{S_T}{S}\right)d\zeta d\eta \tag{25}$$

In order to quantify the effect of nanoparticles volume fraction on convection heat transfer and energy efficiency the following average Nusselt number and entropy generation also defined and calculated:

$$\overline{Nu}^*=\frac{\overline{Nu}(\phi)}{\overline{Nu}(\phi=0)},\quad \overline{S}^*=\frac{\overline{S}(\phi)}{\overline{S}(\phi=0)} \tag{26}$$

3. NUMERICAL SOLUTION

The transformed unsteady Navier-Stokes and energy equations are solved numerically using the control volume approach in a staggered grid arrangement. A second-order upwind scheme is used for the discretization of the convective terms, and a second order central difference is used for the discretization of the diffusion terms. The SIMPLE algorithm is then implemented for pressure and velocity coupling. During the SIMPLE iteration process, the pressure correction method is established to obtain the real velocity field. The set of resulting algebraic equations were solved iteratively and were performed by a couple manner through the block elimination algorithm. Considering the convergence of the numerical results, the under relaxation method is utilized, whereby the following criterion is adopted to secure steady conditions:

$$\sum_{i,j}\left|\Phi_{i,j}^{m+1}-\Phi_{i,j}^{m}\right|\le 10^{-6} \tag{27}$$

where the generic variable Φ represents the set of three variables, *u, v*, or Θ. In the above inequality, the superscripts m indicates the iteration index, and the subscript sequence (*i, j*) denotes the iteration index. The grid independence study is carried out for three different grids namely, 80 × 80, 90 × 90, and 100 × 100 for differentially heated skewed cavity with a skew angle λ = 45◦ at *Ri* = 10, ϕ = 0.05 and *Ha* = 25. Considering simulated accuracy and CPU time in the range of variables, the uniform grid of 90 × 90 is found sufficiently fine to ensure the grid independent solution, and is utilized for all subsequent simulations. The computations are carried out for a time step close to 10^{-3} .

To ensure numerical method credibility, the developed code validate based on some former published results in the literature. Case of lid-driven skewed cavity flow due to pure fluid (ϕ = 0.0) is tested first. Vertical velocity along the horizontal central line obtained by the method developed in this study, Demirdciz *et al*. (1992) and Nayak *et al*. (2015) are compared in Fig. 2(a). As one can remark, an excellent agreement is observed. A second test for the local Nusselt number along the hot wall for a lid-driven square cavity filled with nanofluid ϕ = 10% and with *Ri* = 1, and *Re* = 100

has been conducted. As shown in Fig. 2(b), the computed Nusselt numbers exhibit good agreement with findings of Abu-Nada and Chamkha (2010) and Nayak *et al*. (2015).

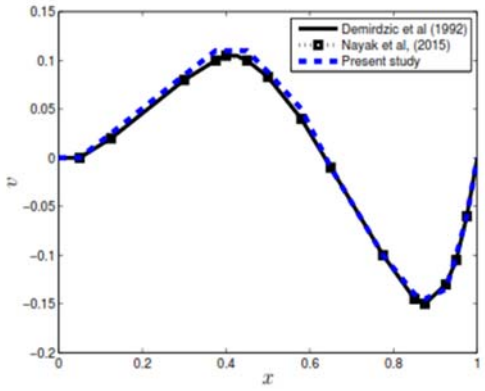

(a)

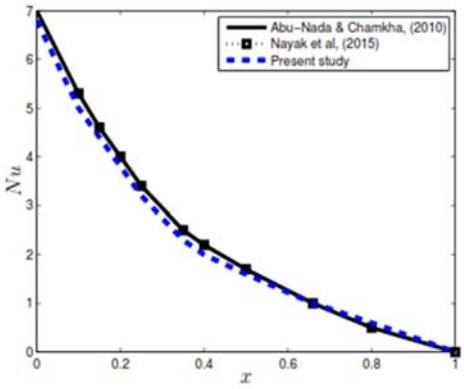

(b)

Fig. 2. (a) Comparison of the present result for *v*-velocity profile with the numerical results due to Demirdzic *et al.* (1992) and Nayak *et al.* (2015), when *Re* = 100, and $\lambda = 45^{\circ}$ for pure fluid ($\phi = 0$) (b) Comparison of the local Nusselt number along the hot wall with former results of Abu-Nada and Chamkha (2010), and Nayak *et al.* (2015), when *Ri* = 1, $\lambda = 90^{\circ}$, and $\phi = 10\%$.

4. RESULTS AND DISCUSSIONS

A numerical examination has been carried out to study MHD natural convection of *Cu*-water nanofluid within a differentially heated skewed lid-driven cavity and in the presence of internal joule heating. Due to the great number of control parameters, all computations carried out by keeping fixed the cavity width (L = 1), the Reynolds number (Re = 100), the Grashof number (Gr = 105), the Hartmann number (Ha = 25), the Prandtl number of the base fluid (Pr = 6.8), the inertial coefficient (C = 0.1), the porosity (ε = 0.9), the viscosity ratio ($R_{\mu} = 1$), the thermal conductivity ratio ($R_k = 1$) ,and irreversibility coefficient ($\chi = 10^{-2}$). The studied parameters are skew angle (λ), Eckert number (Ec), Darcy number (Da), and nanoparticle volume fraction (ϕ). The range of skew angle, Eckert number, Darcy number, and solid volume fraction for this investigation is varied between $30^{\circ} \le \lambda \le 150^{\circ}$, $0 \le Ec \le 0.6$, $10^{-5} \le Da \le 1$, and $0.0 \le \phi \le 0.2$, respectively. The flow field is analyzed through the streamlines, while heat transfer variation is characterized by average Nusselt number at the bottom hot wall. Besides, heat transfer and entropy generation enhancement because of existence metallic nanoparticles is examined by introducing the difference of average Nusselt number and average entropy generation for nanofluid against corresponding pure fluid case. A parametric study on the total entropy generation and Bejan number is also conducted to study the energy efficiency of the system.

4.1 Effect of Darcy Number *Da*

Fig. 3 shows the effect of Darcy number, skew angle and volume fraction of nanoparticles on the streamlines in skewed cavities, when MHD natural convection is provoked by sliding the top lid and vertical temperature difference in one hand and applied constant external magnetic field in the other hand. It is evident that, due to thermal buoyancy and the imposed temperature gradient between horizontal walls, the hot fluid rises up from the hot wall and cold fluid goes down along the cold cross wall. This natural mechanism of convection forms an unicellular clockwise flow pattern, occupied whole the cavity when flow dominated by natural convection. The flow is also influenced by the movement of the lid, due to which fluid flow was stretched to-wards the right wall.

Fig. 3 demonstrates that flow field in a skewed porous cavity is sensible to both skew angle and Darcy number variation. Nayak *et al*. (2015) indicated that with an enhancement of skew angle from 30° to 90°, the effective area of the skewed cavity increases, while with further increase of λ to 150° the effective area of the cavity decreases. Their results also displayed that in the absence of anyexternal magnetic field and in a non-porous media, maximum absolute value of the stream function at the center of the primary vortex ψ_{Max}, increases with skew angle up to λ = 90◦ and then decreased with further increasing of skew angle. The absolute value of the stream function at the center of the primary vortex for all investigated cases in this study registered in Table 2. An almost similar variation in respect to Nayak *et al,* (2015) also observed in this Table, in particular in the first column when ψ_{Max} values of natural convection of Cu-water nanofluid in non-porous media and without external magnetic field registered.

It's clear that both skew angle and Darcy number sufficiently influenced ψ_{Max} values. In order to clarify the matter, the difference of ψ_{Max} value for MHD natural convection in porous media and natural convection in non-porous media calculated and

illustrated as a function of skew angle for various

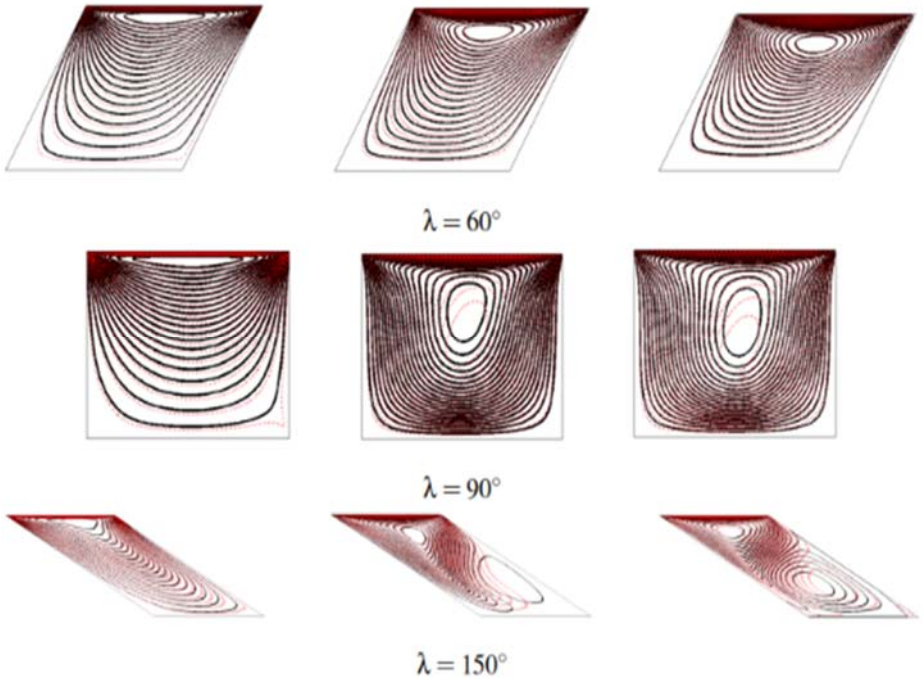

Fig. 3. Streamlines for different skew angle (λ) and solid volume fraction (ϕ) at *Da* = 1 (first column), 10^{-3} (second column), and 10^{-5} (third column), when *Ri* = 10. Dotted lines for pure fluid ($\phi = 0$) and solid lines for nanofluid ($\phi = 6\%$) .

Table 2 Maximum absolute value of stream function at the center of the primary vortex of the cavity ψ_{Max}, for different skew angles and various (a) Darcy numbers, (b) Eckert numbers, and (c) solid volume fractions. All values had to be divided by 10^2

(a)

Skew angle	Ha = 0	ε=0.9, EC= 0.1, ϕ= 0.06 ,Da=			
		1E-4	1E-3	1E-1	1
30^0	8.842	0.9401	4.3784	7.140	7.209
45^0	8.791	1.166	3.547	6.591	6.682
60^0	9.055	1.632	3.161	6.531	6.647
90^0	15.631	0.8808	3.872	6.678	6.724
120^0	10.999	1.808	3.422	5.371	5.423
150^0	6.413	0.9912	2.731	5.011	5.083

(b)

Skew angle	ε=0.9, Da= 10^{-3}, ϕ= 0.06			
	EC=0.0	0.2	0.4	0.6
30^0	4.3784	4.378	4.377	4.376
45^0	3.547	3.547	3.547	3.545
60^0	3.161	3.060	3.588	3.058
90^0	3.872	3.702	3.757	3.57
120^0	3.422	3.427	3.433	3.433
150^0	3.161	3.09	3.071	3.07

(c)

Skew angle	ε=0.9,EC=0.1,Da=10^{-3}				
	ϕ=0.0	0.06	0.1	0.15	0.2
30^0	4.511	4.352	4.318	4.281	4.125
45^0	3.741	3.512	3.487	3.385	3.332
60^0	3.256	3.201	3.112	3.022	2.805
90^0	4.550	3.931	3.514	3.101	2.858
120^0	3.431	3.339	3.276	3.034	2.801
150^0	2.481	2.703	2.611	2.524	2.287

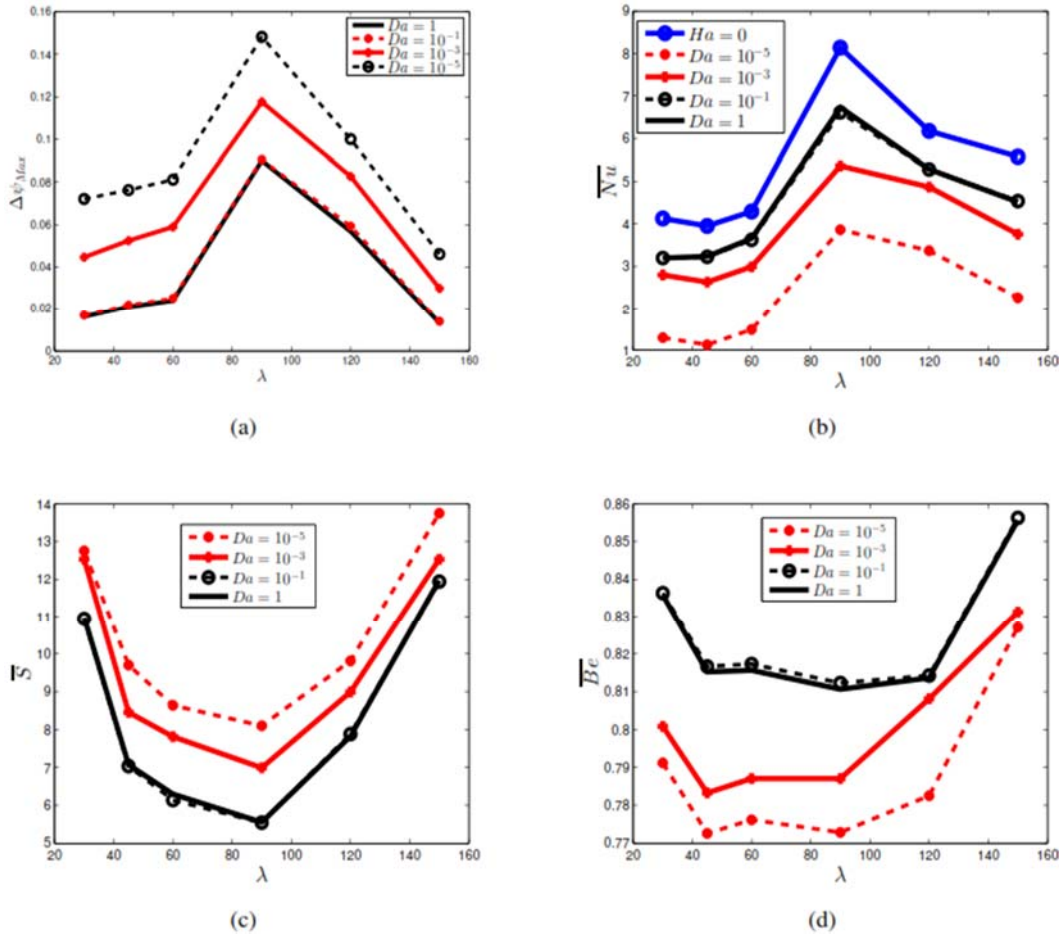

Fig. 4. (a) Variation of maximum absolute value of stream function difference at the center of the primary vortex of the cavity $\Delta\psi_{Max}$, as a function of skew angle for different Darcy numbers. The effect of Darcy number and skew angle on average (b) Nusselt number, (c) entropy generation, and (d) Bejan number, when *Ri* = 10, *Ec* = 0.05, and $\phi = 6\%$.

Darcy number in Fig. 4(a). It is obvious that the intensity of fluid flow is reduced enough in cases with lower Darcy numbers. In the other words, the fluid intensity increases with increasing Darcy number, observed in Table 2(a). Actually, low Darcy number represents low permeability or high flow resistance within the porous bed. Hence, in cases with the low values of Darcy numbers, the intensity of buoyancy driven flow is small due to high flow resistance. This observation is in agreement with earlier results of Bosak *at al*, (2010) on mixed convection flows in a lid-driven porous cavity. On the other hand, Fig. 4(a) shows that cases with $\lambda = 90^{\circ}$ have highest $\Delta\psi_{Max}$ values. This attributes to the effective area of the skewed cavity (Nayak *et al*. 2015), whereby the influence of Darcy number is more pronounced with increasing the effective area of the cavity.

The accentuation of driven buoyancy flow because of further decreasing of Darcy number also observed in fluid patterns, Fig. 3. For $\lambda \le 90^{\circ}$, it can see that the primary vortex which compressed upwards, moves downwards with decreasing Darcy number. For $\lambda > 90^{\circ}$ reducing Darcy number forms secondary eddy near the bottom hot wall. Secondary eddy formation appears as the fluid losses momentum and disappears when the buoyancy driven flow is strong enough. Nayak *et al*. (2015) and Hussain and Hussain (2014) studied mixed convection of nanofluid in a non-porous skewed cavity and observed small secondary eddy at the bottom right corner of a skewed enclosures with $\lambda > 90^{\circ}$. It seems that, secondary eddy formation in porous skewed cavity with $\lambda = 90^{\circ}$ augmented with decreasing Darcy number. Further-more, with an increase of nanoparticle volume fraction, the size of secondary eddy increases. This attributes to the reduction of buoyancy effect as the solid volume fraction of metallic nanopaticles increased.

Heat transfer within the cavity characterized in Fig. 4(b), where average Nusselt number as a function of skew angle for various Darcy numbers illustrated. It should be noted that the average Nusselt number for natural convection (*Ha* = 0) in non-porous media is also presented and named *Ha* = 0. The variation of $\overline{Nu}$ in cases with $Ha = 0$ resembles the result of

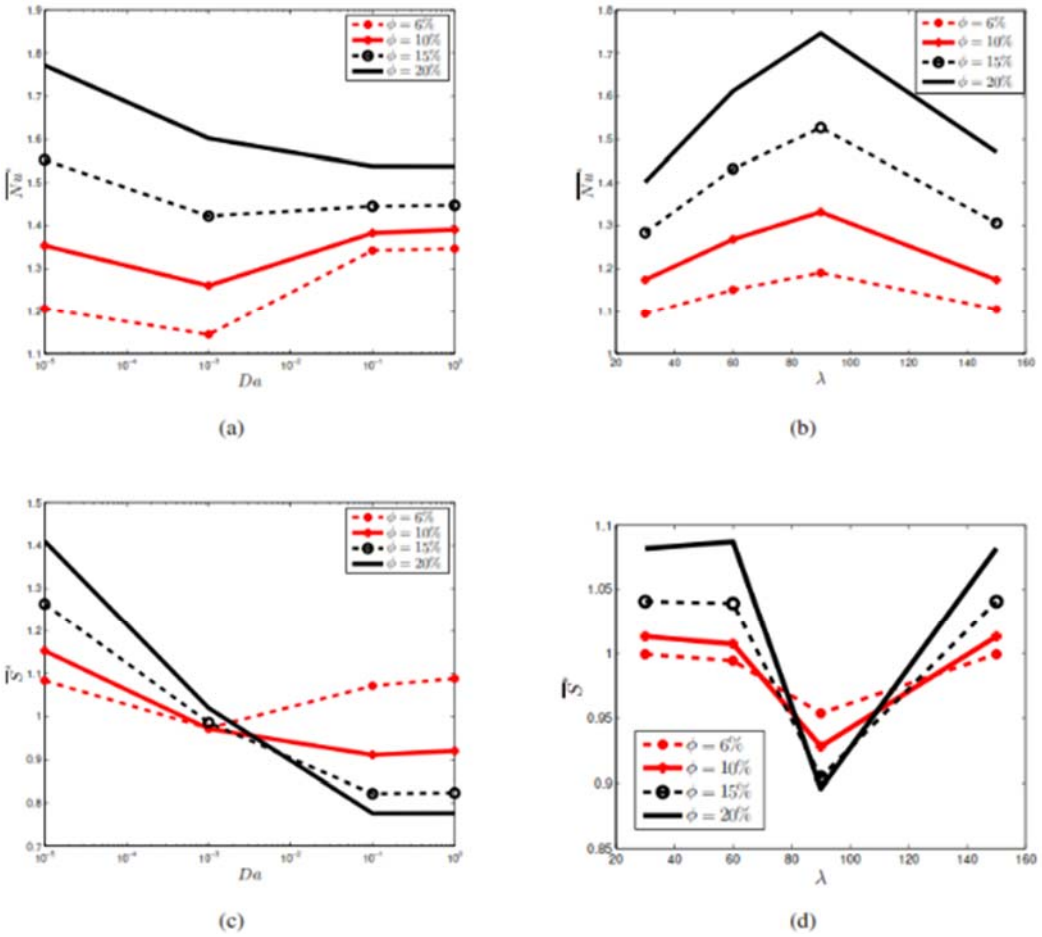

Fig. 5. The effect of solid concentration on the variation of the average Nusslet number and total entropy generation for different values of Darcy number and skew angle.

Nayak *et al*. (2015) and Hussain and Hussain (2014) for a skewed driven cavity filled by nanofluid without external magnetic field. This figure depicted that applying external magnetic field reduced convection heat transfer within the cavity. The resistance effect of Lorentz force against convection heat transfer mode has been shown by many previous investigators (Mejri *et al*. 2014 and 2015, Murthy *et al*. 2013). It can also see that cases with low and moderate permeabilities ($Da = 10^{-5}$ and 10^{-3} , respectively) of the porous medium have smaller $\overline{Nu}$ values, which results in more heat trans-fer reduction caused by low permeability. The average Nusselt number increases with an increase of skew angle for $\lambda < 90^{\circ}$, and attain its maximum value at the skew angle $\lambda = 90^{\circ}$. Furthermore, it decreases with further increase of skew angle. The variation of $\overline{Nu}$ versus inclination angle attributes to the effective area of the skewed cavity. With increase of skew angle from 30° to 90°, effective are enhanced and heat transfer within the cavity improved. However, with further enhancement of the skew angle from, the effective area and so convection heat transfer reduced.

Fig. 4(c) displays the variation of average entropy generation as a function of skew angle. It can see that the trend of $\overline{S}$ values is inverse to that of $\overline{Nu}$ values. This is because of straight relationship of the average entropy generation and effective area of the skewed cavity. With an increase of effective area convection heat transfer increased and so conduction heat transfer mode/thermal irreversibility reduced. Fig. 4(c) also shows that cases with the low and moderate permeabilities of the porous medium have larger $\overline{S}$ values. It was mentioned earlier that low Darcy number denotes low permeability or high flow resistance within the porous bed. Therefore, fluid friction/irreversibility and further entropy generation improved with reducing Darcy number. The variation of average Bejan number as a function of skew angle for various Darcy numbers displays in Fig. 4(d). It can see that the value of $\overline{Be}$ increased with increasing Darcy number. In the other words, with increasing permeability of porous medium, the heat transfer irreversibility dominates the fluid friction irreversibility. It may be noted that with the increase of *Da*, fluid resistance within the porous bed decreases, the buoyancy effect increases for which the irreversibility due to heat transfer increases. This figure also denotes that $\overline{Be}$ has its maximum values

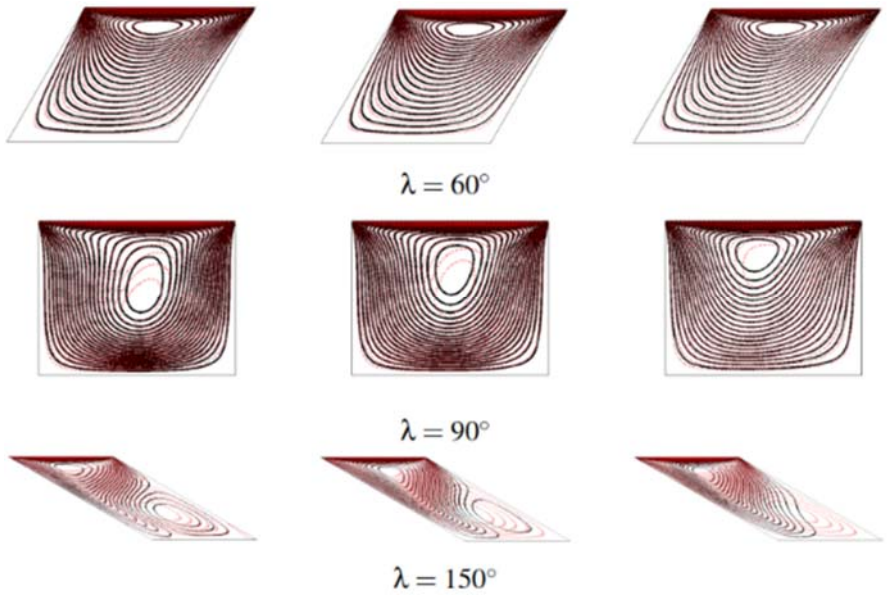

Fig. 6. Streamlines for different skew angle (λ) and solid volume fraction (ϕ) at *Ec* = 0 (first column), 0.2 (second column), and 0.6 (third column), when Ri = 10. Dotted lines for pure fluid ($\phi = 0$) and solid lines for nanofluid ($\phi = 6\%$) .

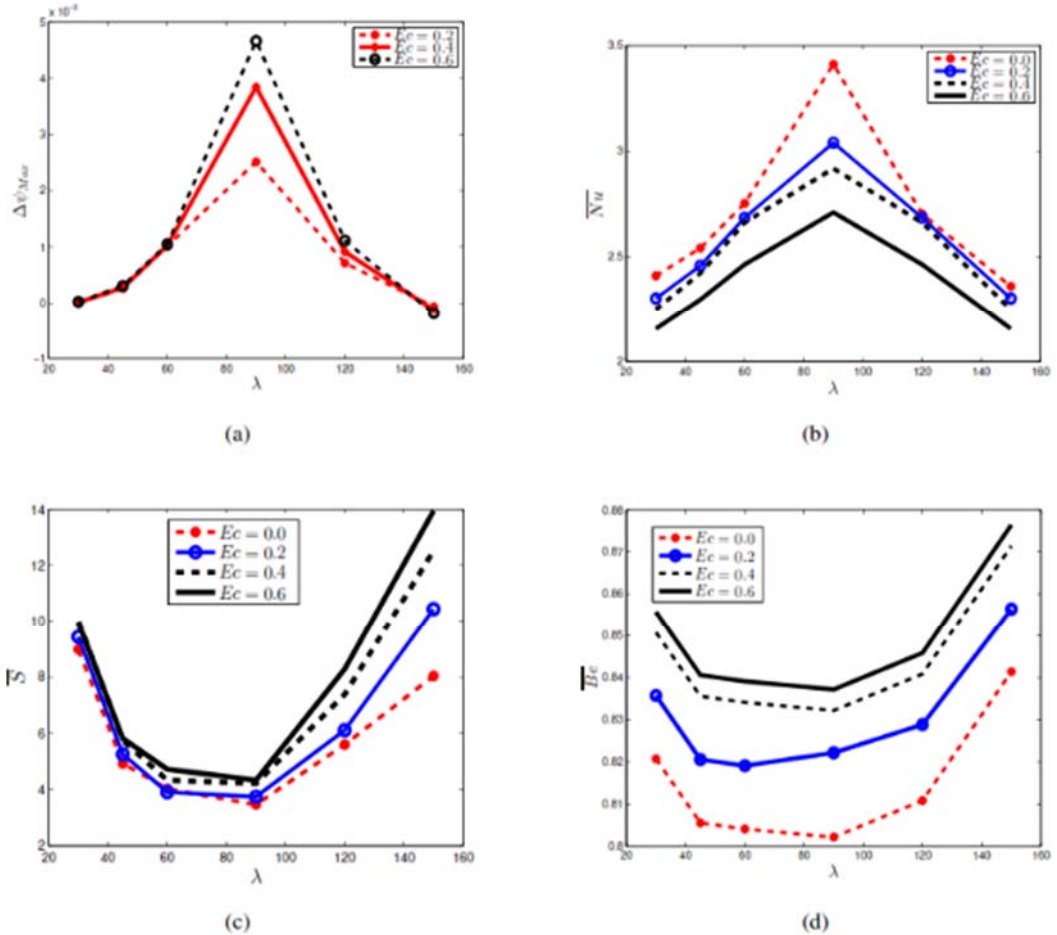

Fig. 7. (a) Variation of maximum absolute value of stream function difference at the center of the primary vortex of the cavity $\Delta\psi_{Max}$ as a function of skew angle for different Eckert numbers. The effect of Eckert number and skew angle on average (b) Nusselt number, (c) entropy generation, and (d) Bejan number, when *Ri* = 10, Da = 10^{-3} , and $\phi = 6\%$.

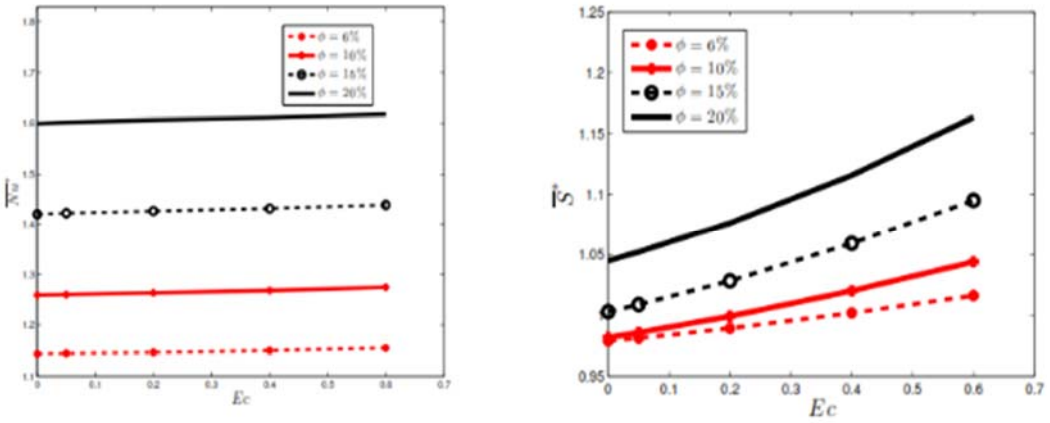

Fig. 8. The effect of solid concentration on the variation of the average Nusslet number and total entropy generation for different values of Eckert number and skew angle.

near the lowest or highest skew angle. This may be due to the fact that at these two extreme value of λ, thermal irreversibility has its highest values.

To characterize the effect of nanoparticles on heat transfer, $\overline{Nu}^*$ illustrated as a function of Darcy number for a certain skew angle ($\lambda = 60^\circ$) and as a function of skew angle for a certain Darcy number ($Da = 10^{-3}$) in Figs. 5(a)and(b), respectively. First, it can see that the existence of metallic nanoparticles make an enhancement in heat transfer, whereby $\overline{Nu}^*$ increased with solid volume fraction. On the other hand, it was explained earlier that reducing Darcy number decreases the intensity of buoyancy force. For this, we find that the heat transfer enhancement in porous media saturated by nanofluid is highest when the buoyancy effect is lowest. Fig. 5(b) shows that heat transfer enhancement rate in nanofluid at a fixed *Da* is almost symmetric about the skew angle $\lambda = 90^\circ$ .The variation of entropy generation ratio as a function of Darcy number for a certain skew angle ($\lambda = 60^\circ$) is displayed in Fig. 5(c). It can see that the existence of metallic nanoparticles increased entropy generation in porous medium with low and moderate permeabilities, while the inverse observed in porous medium with higher permeabilities. It was mentioned earlier that the low Darcy number denotes high fluid friction within the porous bed. Besides, adding nanoparticles increases viscous dissipation and further fluid friction along the cavity. Therefore, adding more metallic nanoparticles in porous media with lower Darcy numbers caused more entropy generation. In contrast, heat transfer enhancement observed in porous media with larger Darcy numbers or larger amount of metallic nanoparticles for the range considerate, i.e. volume fraction up to 20%. Hence, existing nanoparticles in porous media with high permeability reduced thermal irreversibility across the skewed cavity and so decreased entropy generation. Fig. 5(c) depicts the effect of the inclination angle on $\overline{S}^*$ at different values of nanoparticles volume fraction. It can see that in a skewed cavity with $\lambda = 90^\circ$ highest effective area, entropy generation reduced with an increase of nanoparticles volume fraction. This may be caused by increasing convective heat transfer/reducing thermal irreversibility with increasing effective area.

4.2 Effect of Eckert Number *Ec*

The effect of joule heating on fluid flow, heat transfer and fluid irreversibilities of nanofluid in a porous media with a moderate permeability ($Da = 10^{-3}$) is investigated now. Fig. 6 shows the effect of Eckert number on the streamlines of the MHD natural convection in a differentially heated porous skewed lid-driven cavities saturated by nanofluid with various skew angle. For $\lambda < 90^\circ$, the effect of Eckert number on the streamlines seems to be insignificant. For $\lambda = 90^\circ$, the primary vortex moves upwards and becomes smaller with increasing Ec value, which result in increase of heat within the skewed cavity. For $\lambda > 90^\circ$, secondary eddy observed before shrinks with increasing Eckert number which can be again due to increase of heat in the cavity. The effect of nanoparticles existence also observed in this figure, whereby with an increase of nanoparticle volume fraction, the size of secondary eddy sufficiently decreased. Increasing internal joule heating in the presence of high thermal conductive nanoparticles produced more heat in the cavity and accentuated secondary eddy formed by momentum loosing.

The absolute value of steram function at primary vortex for cases with various Eckert number registered in Table 2(b). It can observe that the effect of Ec on steram function values is insignificant. However, the difference of ψ_{Max} for cases with various Eckert numbers and cases without joule heating (*Ec* = 0) illustrated in Fig. 7(a). Cases with either highest Eckert numbers or inclination angle of

$\lambda = 90^{\circ}$ has the largest stream function differences. In fact, the effect of internal joule heating is pronounced with increasing effective area, whereby more heat produced in skewed cavity with larger effective area. The influence of Eckert number and skew angle on heat transfer and entropy generation displayed in Figs. 7(b)and(c), respectively. It is clear that both figures are almost symmetric around $\lambda = 90^{\circ}$. Internal joule heating usually make a distortion in convective current of heat transfer (Rahman *et al*. 2010), and so cases with larger Eckert numbers have smaller $\overline{Nu}$ values. In contrast, internal joule heating increased thermal irreversibility and further make an enhancement in entropy generation. Fig. 7(d) shows the effect of skew angle and internal joule heating on the average Bejan number. For all cases, the value of $\overline{Be}$ is larger than 0.8, which means that thermal irreversibility dominates the fluid friction irreversibility. Moreover, increasing joule heating increased the contribution of thermal irreversibility in entropy generation and so make an enhancement in average Bejan number. The existence of heavy metallic nanoparticles influenced fluid intensity within the cavity. Right columns of Table 2(c) demonstrates that absolute value of the stream functions at primary vortex reduced with increasing solid volume fraction. It is evident that with increase of nanoparticles volume fraction, viscous dissipation and fluid friction increased.

The influence of internal joule heating on ratios of average heat transfer and entropy generation between the nanofluid and pure fluid in porous media is displayed in Fig. 8. The results show that both Nu∗ and S∗ enhanced with increase of Eckert number. In addition, the ratio $\overline{Nu}^{*}$ remains above 1 for all cases considered. It seems that adding more high conductive metallic nanoparticles combine with internal joule heating improved slightly convection heat transfer across the cavity. However, the role of metallic nanoparticles on entropy generation is more pronounced when involved by internal joule heating. It can see that the ratio $\overline{S}^{*}$ is monotonically increased with increasing Eckert number.

5. CONCLUSION

A numerical examination of MHD natural convection in a differentially heated porous lid-drive skewed cavity saturated by Cu-water nanofluid is made in this study. The flow and heat transfer characteristics are illustrated by presenting the stream-lines and average Nusselt number along the heated wall. Analyzes of entropy generation has also been carried out to study the effect of key parameters on fluid irreversibilities. As a disclosure of the present numerical study, the following conclusions can be drawn:

1. It is observed that heat transfer and entropy generation in porous skewed cavity is sensitive enough to the skew angle, Darcy number, and the nanoparticles volume fraction. The average Nusselt number found maximum when $\lambda = 90^{\circ}$, while the average entropy generation is minimum at $\lambda = 90^{\circ}$
2. The obtained results denote that reducing porous medium permeability similar to that of introducing more volume fraction of nanoparticles causing a slowdown of the fluid intensity.
3. At a fixed skew angle, the enhancement ratio of heat transfer compared to the pure fluid case increases with the increase of solid volume fraction for the range considerate, i.e. volume fraction up to 20%.
4. Results indicated that, average entropy generation and Nusselt number of nanofluid in porous media with internal joule heating increased and decreased with further enhancement of Eckert number, respectively.
5. The average Bejan number shows that the contribution of fluid friction irreversibility in entropy generation increased with decreasing either Darcy or Eckert number.

REFERENCES

Abbasian Arani, A. A., M. Mahmoodi and S. Mazrouei Sebdani (2014). On the cooling process of nanofluid in a square enclosure with linear temperature distribution on left wall. *Journal Applied Fluid Mechanics* 7, 591-601.

Abu-Nada, E. and A. J. Chamkha (2010). Mixed convection flow in a lid-driven inclined square en-closure filled with a nanofluid. *Europian Journal of Mechanics B/Fluids* 29, 472-482.

Abu-Nada, E. and A. J. Chamkha (2014). Mixed convection flow of a nanofluid in a lid-driven cavity with wavy wall. *International Communication in Heat and Mass Transfer* 57, 36-47.

Astanina, M. S., M. A. Shermet and J. C. Umavathi (2015). Unsteady natural convection with temperature dependent viscosity in a square cavity filled with a porous medium. *Transport in Porous Media* 110, 113-126.

Basak, T., S. Rey, S. K. Singh and I. Pop (2010). Analysis of mixed convection in a lid-driven porous square cavity with linearly heated side walls. *International Journal of Heat and Mass Transfer* 3, 1819-1840.

Bejan, A. (1979). A study of entropy generation in fundamental convection heat transfer. *ASME Journal of Heat Transfer* 101, 718-725.

Bhattacharya, P. and S. Das (2015). A study on steady natural convective heat transfer inside a square cavity for different values of Rayleigh and Nusselt numbers. *Journal of Applied Fluid Mechanics* 8, 635- 640.

Choi, S. U. S. (1995). Enhancing thermal conductivity of fluid with nanoparticles. *ASME*

Fluid Engineering Division 23, 99-105.

Dehsara, M., N. Dalir and M. R. H. Nobari (2014). Numerical analysis of entropy generation nanofluid flow over a transparent plate in porous medium in presence of solar radiation, viscous dissipation and variable magnetic field. *Journal of Mechanical Science Technology* 28, 1819-1831.

Demirdzic, I., Z. Lilek and M. Peric (1992). Fluid flow and heat transfer test problems for non-orthogonal grids: bench-mark solutions. *International Numerical Methods in Fluids* 15, 329-354.

Fersadou, I., H. Kahalerras and M. El Ganaoui (2015). MHD mixed convection and entropy gen-eration of a nanofluid in a vertical porous channel. *Computers and Fluids* 121, 164-179.

Ghalambaz, M., F. Moattar, M. A. Shermet and I. Pop (2015). Triple-diffusive natural convection in a square porous cavity. *Transport in Porous Media* 111(1), 59-79.

Hussein, S. H. and A. K. Hussain (2014). Natural convection heat transfer enhancement in a differentially heated parallelogramic enclosure filled with copper-water nanofluid. *ASME Journal of Heat Transfer* 136, 82502-82508.

Loganthan, P. and C. Vimala (2015). MHD flow of nanofluids over an exponentially stretching sheet embedded in a stratified medium with suction and radiation effects. *Journal of Applied Fluid Mechanics* 8, 85-93.

Makinde, O. D. (2012). Heat and mass transfer by MHD mixed convection stagnation point flow to-ward a vertical plate embedded in a highly porous medium with radiation and internal heat generation. *Meccanica* 47, 1173-1184.

Malvandi, A., F. Hedayati and M. R. H Nobari (2014). An HAM analysis of stagnation-point flow of nanofluid over a porous stretching sheet with heat generation. *Journal of Applied Fluid Mechanics* 7, 135-145.

Mehrez, Z., A. E. Cafsi, A. Belghith and P. Le Quere (2015). The entropy generation analysis in the mixed convection assisting flow of Cu-water nanofluid in an inclined open cavity. *Advanced Powder Technology* 26(5), 1442-1451.

Mejri, I. and A. Mahmoudi (2015). MHD natural convection in a nanofluid-filled open enclosure with a sinusoidal boundary condition. *Chemical Engineering Research and Design* 98, 1-16.

Mejri, I., A. Mahmoud, M. A. Abbasi and A. Omri (2014). Magnetic field effect on entropy generation in a nanofluid-filled enclosure with sinusoidal eating on both side walls. *Powder Technology* 266, 340-353.

Mohammadi, F. and M. M. Rashidi (2016) Spectral collocation solution of MHD stagnation-point flow in porous media with heat transfer. *Journal of Applied Fluid Mechanics* 9, 773-783.

Moumni, H., H. Welhezi, R. Djebali and E. Sediki (2015). Accurate finite volume investigation of nanofluid mixed convection in two-sided lid-driven cavity including discrete sources. Applied Mathematical Modelling 39, 4164-4179.

Murthy, P. V. S. N., C. Reddy, A. J. Chamkha and A. M. Rashad (2013). Magnetic effect on thermally stratified nanofluid saturated non-Darcy porous mediumum under convective boundary condition. *International Communication in Heat and Mass Transfer* 47, 41-48.

Muthtamilselvan, M. and D. H. Doh (2014). Mixed convection of heat generating nanofluid in a lid-driven cavity with uniform and non-uniform heating of bottom wall. *Applied Mathematical Modelling* 38, 3164-3174.

Muthtamilselvan, M., P. Kandaswamy and J. Lee (2010). Heat transfer enhancement of Copper water nanofluids in a lid-driven enclosure. *Communication in Nonlinear Science and Numerical Simulations* 15, 1501-1510.

Nayak, R. K., S. Bhattacharyya and I. Pop (2015). Numerical study on mixed convection and entropy generation of Cu-water nanofluid in a differentially heated skewed enclosure. *International Journal of Heat and Mass Transfer* 85, 620-634.

Nield, D. A. and A. Bejan (2013). *Convection in porous media*, 4th ed., Springer, New York.

Pekmen, B. and M. Tezer-Sezgin (2014). MHD flow and heat transfer in a lid driven porous enclosure. *Computers and Fluids* 89, 191-199.

Rahman, M. M., M. A. Alim and M. M. A. Sarker (2010). Numerical study on conjugate effect of joule heating and magneto-hydrodynamics mixed convection in an obstructed lid-driven square cavity. *International Journal of Heat Mass and Transfer* 37, 524-534.

Rahman, M. M., S. Mojumder, S. Saha, A. H. Joarder, R. Saidur and A. G. Naim (2015). Numerical and statistical analysis on unsteady magnetohydrodynaimc convection in a semi-circular enclosure filled with ferrofluid. *International Journal of Heat and Mass Transfer* 89, 1316-1330.

Sahoo, S. N., J. P. Panda and G. C. Dash (2013). The MHD mixed convection stagnation point flow and heat transfer in a porous medium. In *Proceedings of National Academy Sciences*, India, Section A Physical Sciences 83, 371-381.

Servati, A. A., K. Javaherdeh and H. R. Ashorynejad (2014). Magnetic field effects on force convection flow of a nanofluid in a channel partially filled with porous media using Lattice Boltzmann Method. *Advanced in Powder Technology* 25, 666-675.

Sheikholeslami, M., M. Hatami and D. D. Ganji (2013). Analytical investigation of MHD

nanofluid flow in a semi-porous channel. *Powder Technology* 246, 327-336.

Shermet, M. A. and I. Pop (2014). Thermo-Bi convection in a square porous cavity filled by Oxytactic microorganisms. *Transport in Porous Media* 103, 191-205.

Shermet, M. A., T. Grosan and I. Pop (2015). Free convection in a square cavity filled with a porous medium saturated by nanofluid using Tiwari and Das nanofluid model. *Transport in Porous Media* 106, 595-610.

Suneetha, S., N. Bhaskar Reddy and V. Ramachandra Prasad (2011). Radiation and mass transfer effects on MHD free convective dissipative fluid in the presence of heat source/sink. *Journal of Applied Fluid Mechanics* 4, 107-113.

Tiwari, R. K. and M. K. Das (2007). Heat transfer augmentation in a two-sided lid-driven differentially heated square cavity utilizing nanofluids. *International Journal of Heat and Mass Transfer* 50, 2002-2018.

Vafai, K. and C. L. Tien (1981). Boundary and inertia effects on flow and heat transfer in porous media. *International Journal of Heat and Mass Transfer* 24, 193-203.